Preliminary Sex-specific Relationships between Peak Force and Cortical Bone Morphometrics in Human Tibiae Subjected to Lateral Loading

Angela L. Harden, Yun-Seok Kang, Randee L. Hunter, Alexander Bendig, John H. Bolte IV, Noah I. Eckstein, Adam G.F. Smith, Amanda M. Agnew

Abstract Tibia fractures are the most common injury in vehicle-to-pedestrian impacts. To provide accurate injury risk predictions, sex differences in tibia properties should be investigated. The objective of this study was to identify the relationship between structural properties and cortical bone morphometric parameters of tibiae in males and females. Ten tibiae were impacted in a 6 m/s lateral-medial 4-point bending scenario to replicate a vehicle-to-pedestrian blunt impact to the leg. Prior to testing, total length, maximum diameter, medial-lateral diameter, and mechanical span measurements were taken. Total area (Tt.Ar), cortical area (Ct.Ar), cortical thickness (Ct.Th), robustness (Tt.Ar/Length), area moment of inertia (I), and volumetric bone mineral density (vBMD) were calculated from quantitative computed tomography (QCT) scans at 50% of total tibial length (i.e., fracture location). Peak force for the sample ranged from 12.5–21.9 kN (females: 12.5–21.9 kN; males: 12.7–20.2 kN). Peak force values were not significantly different between females and males. Overall, males demonstrated larger cortical bone gross and cross-sectional morphometric values than females. Overall, these results suggest that utilizing cortical bone morphometrics instead of body size-scaling may contribute to increasing the accuracy of the biomechanical response in finite element simulations.

Keywords Cross-sectional geometry, Leg injury, Pedestrian, Tibia fracture.

I. INTRODUCTION

In 2018, 6,283 pedestrians were killed in traffic crashes in the United States, a 3.4% increase from 2017 [1]. In 2017, an estimated 137,000 pedestrians were treated in emergency departments for non-fatal injuries related to motor vehicle crashes [2–3]. The most frequently injured region in a pedestrian versus vehicle crash is the lower extremity, with tibia fractures being the most common injury [4]. The tibia is also a frequent site of fractures in motorcycle crashes, sports injuries, and high-speed activities (e.g., skiing) [5–6]. While tibia fractures are not typically fatal, lower extremity injuries can cause long-term pain and osteoarthritis, which have been correlated with poorer functional outcomes [7–8]. Additionally, individuals who sustained tibial shaft fractures were demonstrated to have higher mortality rates one year post-injury when compared to the general population [7]. The socioeconomic impacts on pedestrians injured in traffic crashes can be profound, specifically within the first year after injury [9–10]. As the trend of pedestrians involved in motor vehicle crashes increases, the need for understanding fracture risk factors increases as well.

The current technique for differentiating tibial responses between females and males is to normalize responses to a standard anthropometry (i.e., females are similar but smaller versions of males) [11–12]. However, previous studies have demonstrated sex-specific effects of age and body size on tibia cortical bone morphometrics, critical components of bone strength and fracture risk [13–15]. Significant differences in the way males and females develop and lose cortical bone exist across the skeleton [16–19], likely influencing skeletal response to loading. Therefore, conducting pedestrian impact simulations based on the sex and body size of an individual, developed via size-based scaling methods, may not capture the realistic response of a specific element, let alone the whole-body response. To provide accurate injury thresholds, sex differences in tibia properties (biomechanical responses and cortical bone parameters) should be investigated. The objective of this study was to identify the

A. L. Harden (e-mail: angela.harden2@osumc.edu; tel: +1-614-247-8008 is a Research Assistant Professor at The Ohio State University in Columbus, Ohio, USA. A. L. Harden, Y. S. Kang, R. L. Hunter, A. Bendig, J. H. Bolte IV, N. I. Eckstein, A. G. F. Smith, and A. M. Agnew are all affiliated with the Injury Biomechanics Research Center (IBRC), The Ohio State University, USA.

relationship between peak force and cortical bone morphometric parameters of dynamically impacted tibiae in males and females.

II. METHODS

Materials

Ten tibiae from adult males and females were ethically obtained through The Ohio State Body Donation Program, Columbus, Ohio, USA, following compliance protocols established by research ethics advisory committees (Table I). Additional data for each postmortem human subject (PMHS) (e.g., stature, weight, BMI) are provided in Table AI. All tibiae were pre-screened via imaging and visual inspection methods to determine the presence of any pre-existing trauma. Tibiae with any observed trauma to the diaphysis were excluded from this sample. Sample demographics are provided in Table I. All soft tissue was removed from the tibiae, with the exception of the periosteum, which was left intact. All tibiae were then wrapped in normal saline-soaked gauze and stored at -20°C until testing. This storage process does not significantly affect the mechanical properties of cortical bone [20–24].

TABLE I
DESCRIPTIVE STATISTICS OF THE SAMPLE DEMOGRAPHICS

Sex	N	Minimum (years)	Maximum (years)	Mean (years)	SD (years)
Females	5	84	102	89.2	7.4
Males	5	63	77	70.2	6.3

Pre-Test Data Collection

Prior to testing, whole bone computed tomography (CT) scans of each tibia were obtained using a Phillips Ingenuity 64-slice digital PET/CT with consistent acquisition parameters (120 kV; 262 mAs; 1024x1024 matrix; 0.67 slice thickness) resulting in a 0.335 mm in-plane resolution. A Bone Density Calibration Phantom (BDX/6-QRM, Möhrendorf, Germany) with rods of known calcium hydroxyapatite densities (0–800 mg/cm^3) was included in each scan to construct scan-specific calibration curves for vBMD quantification. Skyscan CTAn (Bruker) software was used to quantify cortical bone morphometric parameters (Table II) from a 6.7 mm volume of interest (VOI) at the 50% site of each tibia (Fig. 1).

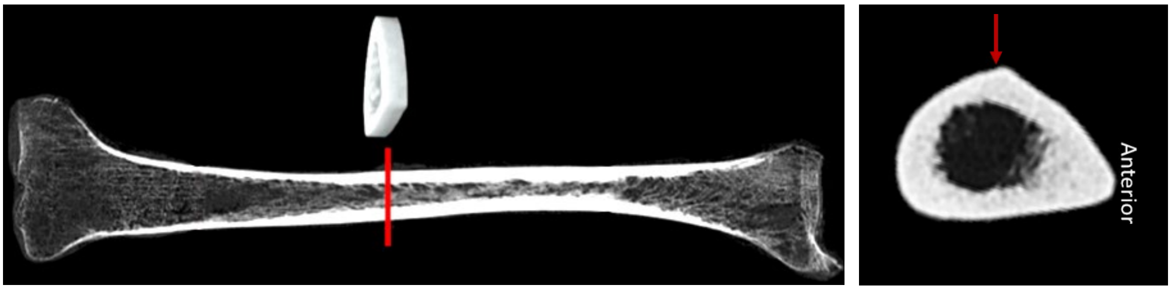

Fig. 1. Exemplar image of QCT scan with 50% volume of interest (VOI) designated with red line and inset image (left) and 50% cross-sectional image (right) with impact direction (red arrow).

TABLE II
CORTICAL BONE MORPHOMETRIC VARIABLES AND DEFINITIONS

Variable (abbreviation, units)	Definition
Total Area (Tt.Ar, mm^2)	Total cross-sectional area
Robustness (R, mm)	Tt.Ar/Total Length
Cortical Area (Ct.Ar, mm^2)	Area between periosteal and endosteal borders
Cortical Thickness (Ct.Th, mm)	Mean distance from periosteal to endosteal border calculated by the annular (derived) method
Area Moment of Inertia (I, mm^4)	Measure of resistance to bending
Volumetric Bone Mineral Density (vBMD, mg/cm^3)	Calculated from scan-specific calibration curves from QRM phantom and using threshold values to isolate cortical bone

Experimental Testing

All tibiae were impacted in a dynamic 6 m/s lateral-medial 4-point bending scenario to replicate a vehicle-to-pedestrian blunt impact to the leg. Fractures of the tibial shaft are the most common of all diaphyseal fractures [25], specifically, injuries are more common in the middle and distal portions [6][26]. Therefore, all controlled experimental blunt force trauma testing in this study was conducted on the mid-diaphyseal region of the human tibia. Prior to testing gross measurements of each tibia were collected, including total length (maximum length excluding the medial malleolus), maximum diameter (measured at the nutrient foramen), and medial-lateral diameter (measured at the nutrient foramen). The proximal and distal ends of the tibiae were rigidly potted using Master Dyna-Cast Fast-Cast Urethane (Freeman Manufacturing and Supply Co., Avon, OH, USA) at the 20% and 80% sites, determined based on the total length of the tibia without the medial malleolus, in a custom potting fixture (Fig. 2). To ensure that all tibiae were potted in the same orientation, an anatomically relevant coordinate system was utilized [27]. After potting, mechanical span (pot center to pot center) was measured and tri-axial rectangular rosette (CEA-06-062UR-350, Micro-Measurements, VPG, Raleigh, NC, USA) and uni-axial linear (C4A-06-060SL-350-39P, Micro-Measurements, VPG, Raleigh, NC, USA) strain gages were attached to the diaphysis on the medial, lateral, and posterior surfaces. Rosette strain gages were affixed on the proximal diaphysis at the 55% sites of each surface and uni-axial linear strain gages were mounted on the distal diaphysis at the 45% sites of each surface (Fig. 2) to determine time of fracture.

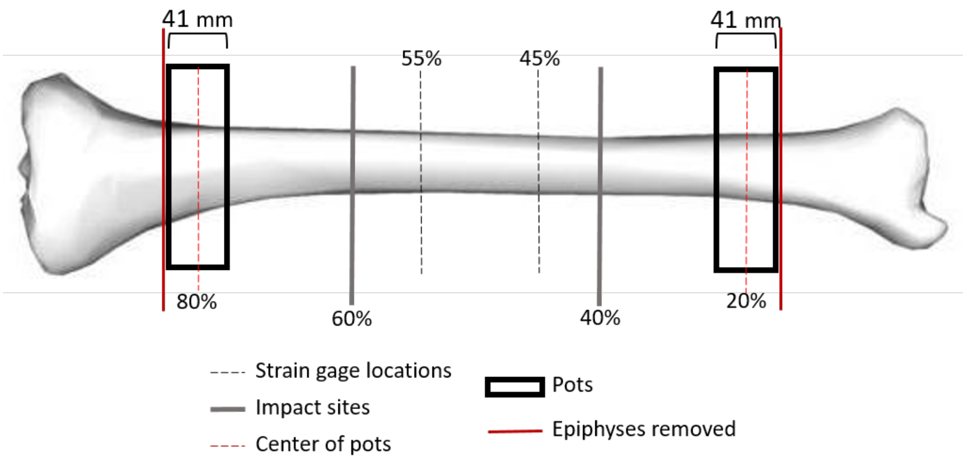

Fig. 2. Schematic of pots, strain gage, and impact locations on a right tibia in testing position (view of posterior surface).

The testing utilized a custom-built material testing system (High Strain-Rate Material Testing System, MTS Systems Corporation, Eden Prairie, MN, USA) equipped with an adjustable impactor, designed to impact the tibiae at the 40% and 60% sites simultaneously (Fig. 3) [28–29]. The anatomical coordinate system, outlined in SAE J211, was utilized, where positive X was anterior, positive Y was lateral for the right tibia and medial for the left tibia, and positive Z was inferior (Fig. 3) [30]. The testing fixture was equipped with two six-axis load cells (Bertec Corporation, Columbus, OH, USA) beneath supported tibia ends and allowed for rotation and translation of both ends. The on-board high-rate MTS data acquisition (BNC-2090, National Instruments, Austin, TX) and an external high-rate data acquisition system (DTS SLICE PRO, Seal Beach, CA, USA) collected data at a sampling frequency of 20,000 Hz and 100,000 Hz, respectively.

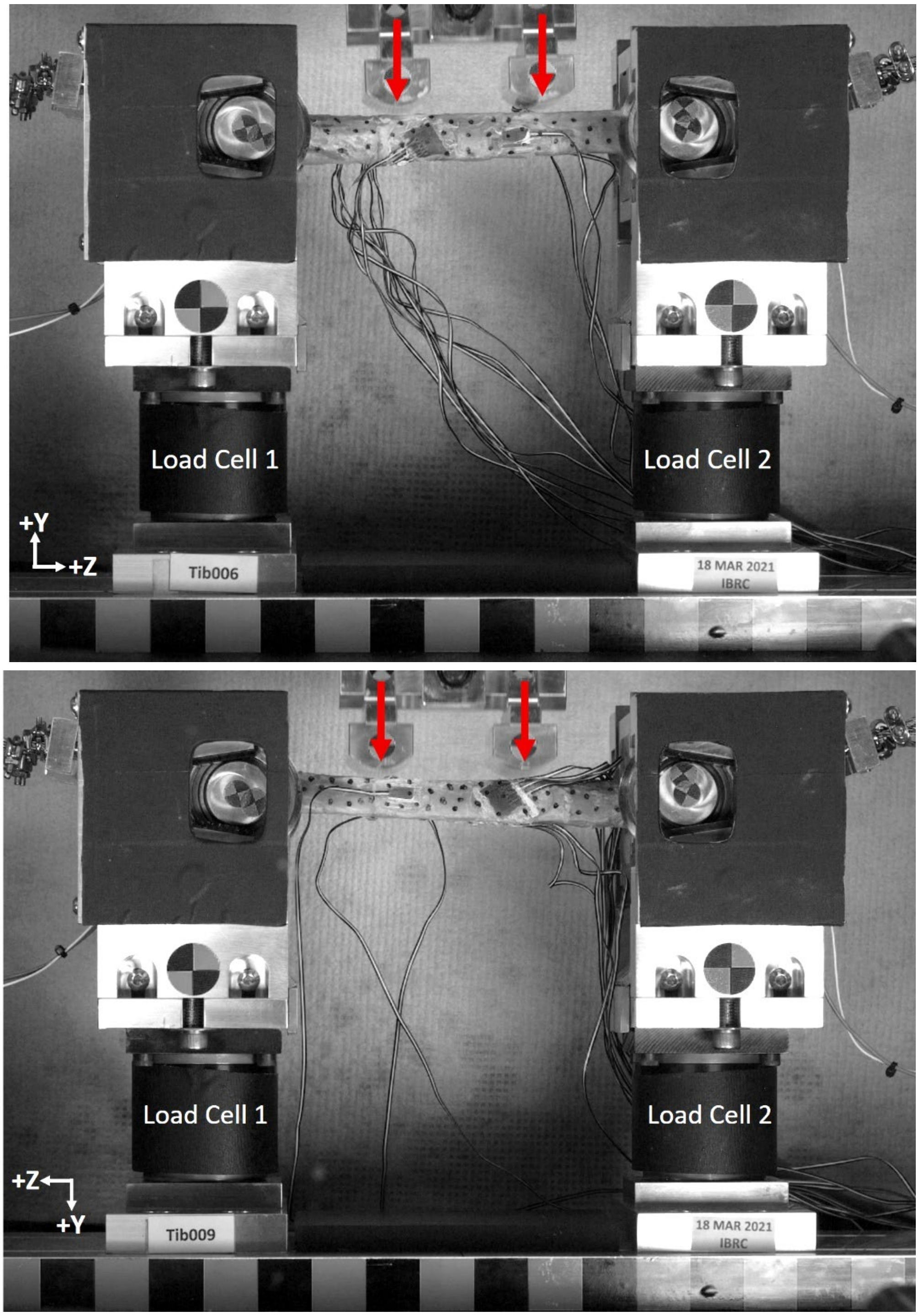

Fig. 3. Exemplars of right tibia (top) and left tibia (bottom) in testing fixture. Coordinate systems are provided for each side (right or left) and red arrows indicate direction of impact.

Data Analyses

Peak force in the primary loading direction (Y) was calculated as the peak of the sum of absolute force data from each load cell (Fig. 4). Peaks were identified from raw data (no filter was used). All variables were tested for normality via the Anderson-Darling test for normality. Scatterplots and linear regressions were utilized to examine the relationships between peak force and gross and cortical bone morphometric parameters. Independent-samples t-tests were used to evaluate sex differences in force, gross measurements, and cortical bone morphometric values. All statistical analyses were performed using Minitab 18 Statistical Software [31] and the significance level for all analyses was α=0.05.

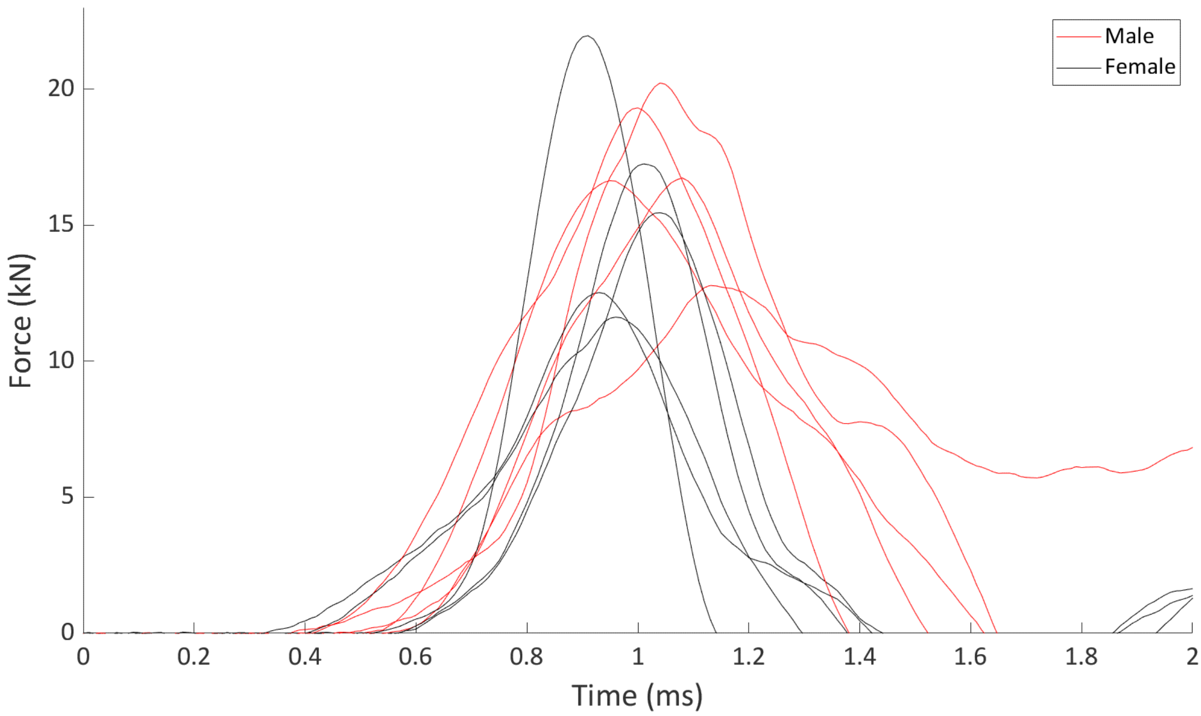

Fig. 4. Peak force-time plot for each tibia (n=10). Female tibiae are indicated in gray and male tibiae are indicated in red.

III. RESULTS

All variables were normally distributed ($p>0.075$). Sex-specific descriptive statistics and independent-samples t-tests results are provided in Table III. Peak force in Y for the entire sample ranged from 12.5–21.9 kN, females ranged from 12.5–21.9 kN and males ranged from 12.7–20.2 kN (Fig. 4, A1–A10). Females and males did not demonstrate significant differences in peak force values ($p=0.991$). Females and males exhibited similar ranges of peak force, with females exhibiting a slightly larger value range than males. Males demonstrated larger mean values for all gross measurements, with significant differences observed between sexes for all variables ($p<0.022$), except for medial-lateral diameter ($p=0.617$). Males demonstrated larger values for all cortical bone morphometrics, with significant differences observed between sexes in all parameters ($p<0.049$), except R ($p=0.260$) and vBMD ($p=0.335$), at the 50% site of the tibiae (i.e., approximate fracture location) (Table IV). Overall, scatterplots and linear regressions demonstrated no significant relationships between peak force and gross measurements (Table IV, Figs 5–8) or cortical bone morphometric parameters (Table IV, Figs 9–14).

TABLE III
SEX-SPECIFIC DESCRIPTIVE STATISTICS AND INDEPENDENT-SAMPLES T-TEST RESULTS

Variable (unit)	Sex (n)	Minimum	Maximum	Mean	SD	p-value*
Peak Force (kN)	F (5)	12.5	21.9	17.1	3.5	0.991
	M (5)	12.7	20.2	17.1	2.9	
Total Length (mm)	F (5)	326	351	343.4	10.1	**0.022**
	M (5)	355	406	380.2	22.9	
Maximum Diameter (mm)	F (5)	32	35	33.6	1.3	**0.009**
	M (5)	34	38	37.2	1.7	
Medial-Lateral Diameter (mm)	F (5)	22	28	24.0	2.3	0.617
	M (5)	21	27	24.8	2.4	
Mechanical Span (mm)	F (5)	194	209	202.8	6.0	**0.016**
	M (5)	210	243	255.4	12.6	
Tt.Ar (mm^2)	F (5)	362.7	460.4	411.3	35.7	**0.049**
	M (5)	387.4	542.9	488.5	60.7	
R (mm)	F (5)	1.05	1.35	1.22	0.10	0.260
	M (5)	1.11	1.41	1.31	0.12	
Ct.Ar (mm^2)	F (5)	211.5	273.8	237.6	25.0	**0.007**
	M (5)	305.5	426.4	355.3	53.5	
Ct.Th (mm)	F (5)	2.41	4.07	3.30	0.68	**0.008**
	M (5)	4.12	6.10	5.00	0.78	
I (mm^4)	F (5)	12876	18770	15270	2226	**0.024**
	M (5)	17704	36554	28556	8047	
vBMD (mg/cm^3)	F (5)	1083.5	1227.2	1162.3	56.6	0.335
	M (5)	1144.3	1257.6	1196.0	45.9	

*Significant p-values are **bolded**

TABLE IV
LINEAR REGRESSION ANALYSES AND RESULTS

Analysis	Regression Equation	R^2 (%)	p-value
Peak Force vs Total Length	29.44 – 0.03397 Total Length	8.18	0.423
Peak Force vs Maximum Diameter	12.69 + 0.1261 Maximum Diameter	1.00	0.783
Peak Force vs Medial-Lateral Diameter	23.97 – 0.2797 Medial-Lateral Diameter	4.55	0.554
Peak Force vs Mechanical Span	29.55 – 0.05790 Mechanical Span	8.32	0.419
Peak Force vs Tt.Ar	18698 – 3.44 Tt.Ar	0.49	0.847
Peak Force vs R	13151 + 3146 R	1.52	0.735
Peak Force vs Ct.Ar	15968 + 3.98 Ct.Ar	0.93	0.791
Peak Force vs Ct.Th	14167 + 718.4 Ct.Th	7.19	0.454
Peak Force vs I	17441 – 0.0133 I	0.15	0.914
Peak Force vs vBMD	- 2766 + 16.89 vBMD	8.25	0.421

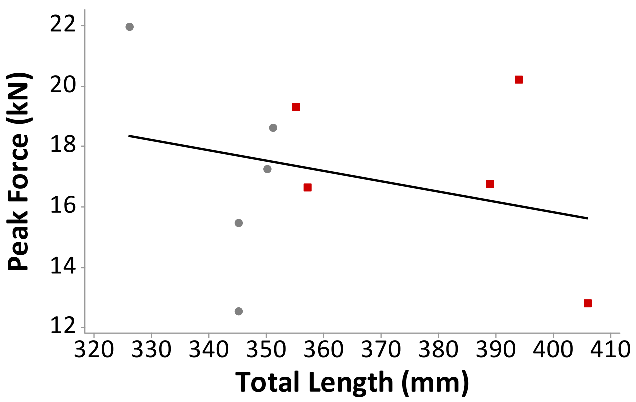

Fig. 5. Scatterplot of Peak Force versus Total Length by sex (females [gray], males [red]) with linear regression line for the entire sample (R^2=8.18%)

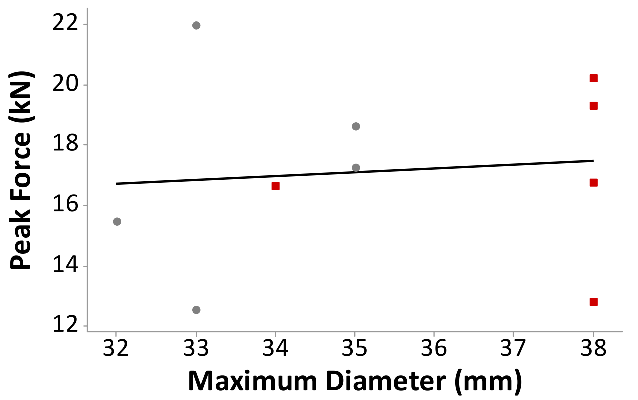

Fig. 6. Scatterplot of Peak Force versus Maximum Diameter by sex (females [gray], males [red]) with linear regression line for the entire sample (R^2=1.00%)

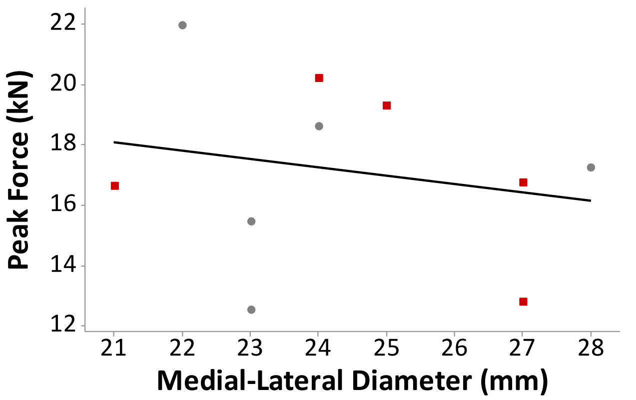

Fig. 7. Scatterplot of Peak Force versus Medial-Lateral Diameter by sex (females [gray], males [red]) with linear regression line for the entire sample (R^2=4.55%)

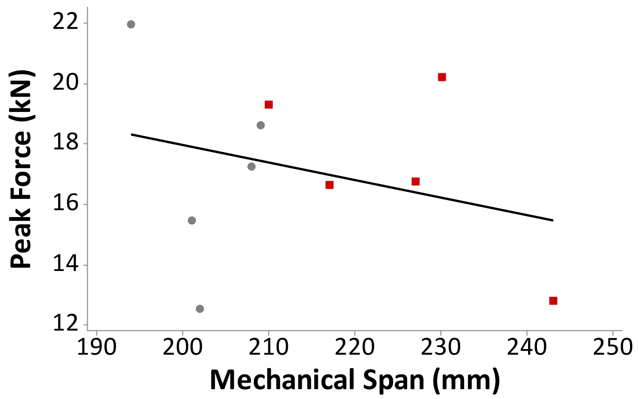

Fig. 8. Scatterplot of Peak Force versus Mechanical Span by sex (females [gray], males [red]) with linear regression line for the entire sample (R^2=8.32%)

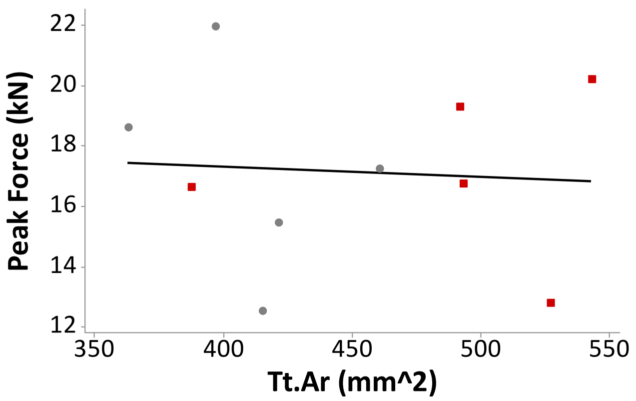

Fig. 9. Scatterplot of Peak Force versus Tt.Ar by sex (females [gray], males [red]) with linear regression line for the entire sample (R^2=0.49%)

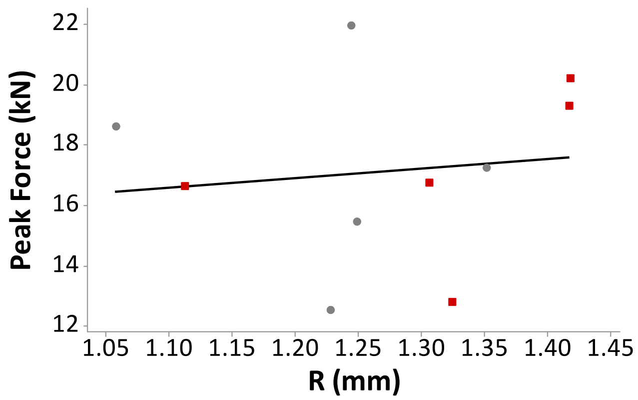

Fig. 10. Scatterplot of Peak Force versus R by sex (females [gray], males [red]) with linear regression line for the entire sample (R^2=1.52%)

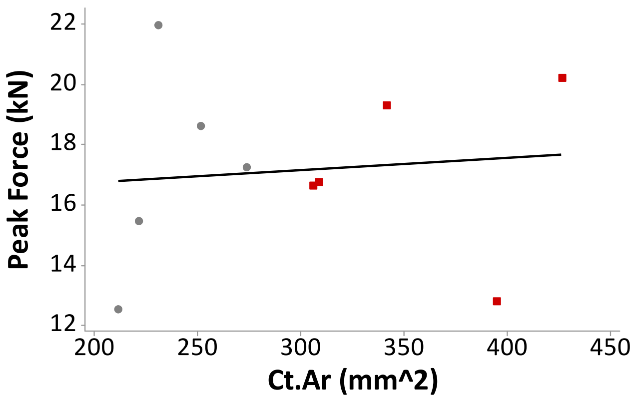

Fig. 11. Scatterplot of Peak Force versus Ct.Ar by sex (females [gray], males [red]) with linear regression line for the entire sample (R^2=0.93%)

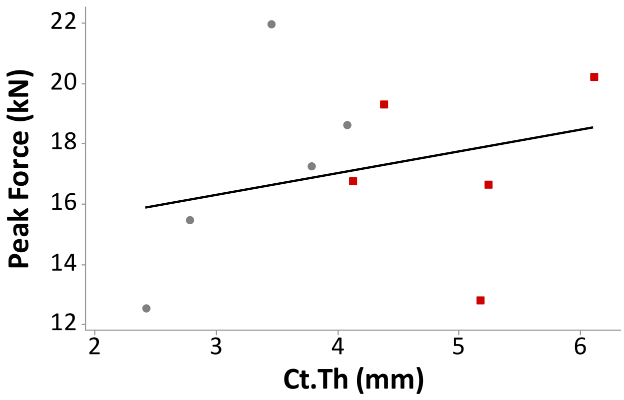

Fig. 12. Scatterplot of Peak Force versus Ct.Th by sex (females [gray], males [red]) with linear regression line for the entire sample (R^2=7.19%)

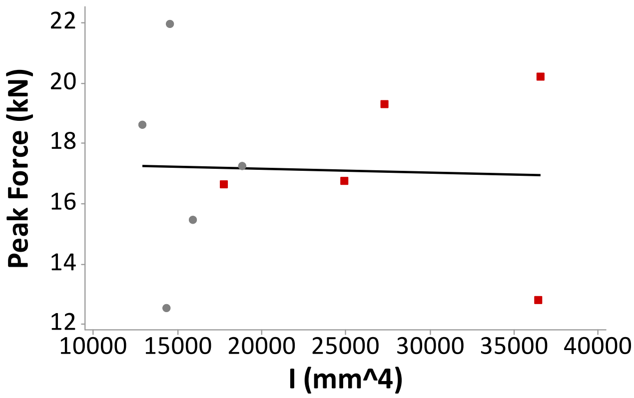

Fig. 13. Scatterplot of Peak Force versus I by sex (females [gray], males [red]) with linear regression line for the entire sample (R^2=0.15%)

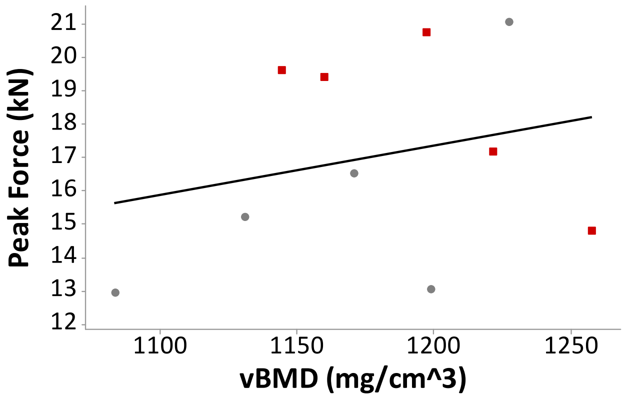

Fig. 14. Scatterplot of Peak Force versus vBMD by sex (females [gray], males [red]) with linear regression line for the entire sample (R^2=8.25%)

IV. Discussion

Peak force values were similar between males and females (p=0.991); however, there was a large amount of variation in force within the sample (Table III, Fig. 4). Overall, male tibiae exhibited larger gross measurements and cortical bone morphometric values than females (Table IV). These findings are consistent with [32], which found that sexual dimorphism affects tibia morphology. Cortical bone morphometric relationships between sexes are consistent with previous studies on larger samples [18][32–33]. No direct comparison of the peak force data is available as previous studies utilized fleshed legs (tibia, fibula, and soft tissue), different loading rates (1.45–4.2 m/s), and/or 3-point bending (instead of the 4-point bending utilized in this study), all of which may affect peak force values [34–37]. Similar to the results from this preliminary study, Tommasini *et al.* [32] demonstrated that material properties (modulus, yield strain, yield stress, post-yield strain, failure strain, and energy-to-failure) were not significantly different between females and males. Interestingly, the largest force value within this sample was for a female subject, even with the female sample being significantly older than the male sample, further suggesting that techniques scaling male data to female data would fail to capture the variation observed in the bony response of females. Furthermore, it would be expected that older females would exhibit lower force values than males; thus, future work will evaluate these relationships within a larger, age-matched sample. Significant sex differences in total length, maximum diameter, mechanical span, Tt.Ar, Ct.Ar, Ct.Th, and I highlight the overall size differences between females and males. However, many maximum female values tended to overlap with minimum male values. These results and observations support the need to incorporate tibia measurements and cortical bone morphometrics, rather than simple sex scaling, in finite element (FE) simulations and injury predictions. As both the lowest and highest peak force values were associated with female tibiae, the current preliminary data suggest that simply assuming a lower injury threshold for force in female tibiae may not be appropriate but more experimental data are required to confirm these preliminary findings.

Previous studies have shown that even after adjusting for body size and robustness, females have lower cortical area values than males [17][38–39], which demonstrates the deficit in techniques of scaling male data to represent females. Milgrom *et al.* [40] found that area moment of inertia was significantly correlated with the incidence of stress fractures in the tibia, and individuals with lower values of I were found to have higher stress fracture morbidity than those with higher values. While robustness was not significantly different between sexes in this preliminary study, females did exhibit lower cortical bone morphometric parameters than males. However, in this preliminary study cortical bone morphometric parameters were unable to predict peak force values. Tibia measurements were also unable to predict peak force values (Table IV). The similar medial-lateral values may be contributing to the comparable peak force values between males and females. This lack of predictability could indicate that additional predictor variables need to be investigated and that further analyses of the combination of gross and cortical bone morphometric parameters in multivariate analyses should be conducted. Since peak force was not significantly different between sexes but most of the gross measurements and cortical bone morphometric parameters were, further investigation into interactions and covariation between these variables and other structural properties or structural responses (e.g., bending moment) at failure, to identify the most accurate prediction model for sex-specific biomechanical responses, is warranted.

There are some limitations within this study that should be addressed. While all subjects were elderly, the age distribution for males and females was significantly different for this preliminary sample (n=10) (p=0.003) (females: mean 89.2 ± 7.4 years; males: mean 70.2 ± 6.3 years). However, previous studies evaluating bone morphometrics in the tibiae have found similar results for age-matched samples [33]. Additionally, [15] found that R, Tt.Ar, and Ct.Ar did not change significantly with age across multiple tibial sites (25%, 38%, 50%, 66%, and 75%). This suggests that the results in this study were not influenced by the differences between the ages of the female and male subjects. The small sample size (n=10) is also a limitation of this study. Future work will increase the size and age range of the sample, likely expanding the variation present in the sample in order to better elucidate sources of variation in peak force. Future work should also evaluate tibia loading and additional structural properties at varying cortical sites, as previous work has suggested that tibia tolerances should be developed for different impact locations [41]. This avenue of research is further supported by [27], which demonstrated that cortical bone morphometrics varied between locations along the length of the tibia (38%, 50%, 66% sites).

V. CONCLUSION

The absence of sex differences in force values and significantly larger values for most male gross measurements and cortical bone morphometric parameters demonstrate the importance of utilizing bone-specific parameters, rather than simply sex, for injury predictions. While peak force was not significantly different between sexes, females represented both the lowest and highest force values, which indicates that scaling male data to female data may fail to capture the full range of responses from female tibiae. Furthermore, based on data from this sample, a lower injury threshold for females should not be assumed. Overall, these results suggest that utilizing tibia-specific measurements and cortical bone morphometrics instead of size-scaling may contribute to increased accuracy of biomechanical response predictions. Further exploration of the preliminary data presented here, with a larger sample size and additional experimental data, are necessary to confirm these findings and to provide more detailed interpretations.

VI. ACKNOWLEDGEMENTS

We are indebted to the anatomical donors for their generous gifts, which make this research possible. Funding for this work was provided by the National Institute of Justice, USA. The views expressed within are solely those of the authors and do not represent the opinions of any sponsors. Thank you to all of the staff and students of the IBRC, The Ohio State University, USA, for all of their support and contributions.

VII. REFERENCES

[1] National Center for Statistics and Analysis (2019) 2018 fatal motor vehicle crashes: Overview. Traffic Safety Facts Research Note. Report No. DOT HS 812 826), 2019.

[2] Centers for Disease Control and Prevention (2017) “Pedestrian Safety” Internet: [https://www.cdc.gov/transportationsafety/pedestrian_safety/], 2017. [Accessed 29 March 2021].

[3] Center for Disease Control and Prevention (2015) “WISQARS (Web-based Injury Statistics Query and Reporting System)” Internet: [http://www.cdc.gov/injury/wisqars], 2015 [Accessed 26 March 2021].

[4] Paas, R., Huber, R., et al. (2018) Pedestrian Leg Injury Distribution in German in-depth Accident Study for Leg Impactor Development. *Proceedings of IRCOBI Conference*, 2018, Athens, Greece.

[5] Murphy, J., Nyland, J., Lantry, J., Roberts, C. (2009) Motorcyclist ‘biker couples’; A descriptive analysis of orthopaedic and non-orthopaedic injuries. *Injury*, 2009, **40**: pp.1195–1199.

[6] Wedel, V. L., Galloway, A. (Eds) (2014) Broken Bones: Anthropological Analysis of Blunt Force Trauma, 2nd Edition. *Charles C Thomas*, Springfield, IL, USA, 2014.

[7] Connelly, C. L., Bucknall, V., et al. (2014) Outcome at 12 to 22 years of 1502 tibial shaft fractures.” *The Bone and Joint Journal*, 2014, **96B**(10): pp.1370–1377.

[8] Milner, S. A., Davis, T. R. C., Muir, K. R., Greenwood, D. C., Doherty, M. (2004) Long-Term Outcome after Tibial Shaft Fracture: Is Malunion Important?. *The Journal of Bone and Joint Surgery*, 2004, **86**(2): pp.436–437.

[9] O’Hara, N. N., Isaac, M., Slobogean, G. P., Klazinga, N. S. (2020) The socioeconomic impact of orthopaedic trauma: A systematic review and meta-analysis. *PLoS One*, 2020, **15**(1): pp.1–22.

[10] Carter, E. L., Neal-Sturgess, C. E., Hardy, R. N. (2008) APROSYS in-depth database of serious pedestrian and cyclist impacts with vehicles. *International Journal of Crashworthiness*, 2008, **13**(6): pp.629–642.

[11] Eppinger, R. H., Marcus, J. H., Morgan, R. M. (1984) Development of Dummy and Injury Index for NHTSAs Thoracic Side Impact Protection Research Program. SAE Technical Paper, 1984.

[12] Mertz, H., Irwin, A., Melvin, J., Stanaker, R., Beebe, M. (1989) Size, Weight and Biomechanical Impact Response Requirements for Adult Size Small Female and Large Male Dummies. SAE Technical Paper, 1989.

[13] Schmidutz, F., Milz, S., *et al.* (2021) Cortical parameters predict bone strength at the tibial diaphysis but are underestimated by HR-pQCT and µCT compared to histomorphometry. *Journal of Anatomy*, 2021, **238**(3): pp.669–678.

[14] Ohlsson, C., Sundh, D., *et al*. (2017) Cortical bone area predicts incident fractures independently of areal bone mineral density in older men. *Journal of Clinical Endocrinology and Metabolism*, 2017, **102**(2): pp.516–524.

[15] Jepsen, K. J., Centi, A., *et al*. (2011) Biological constraints that limit compensation of a common skeletal trait variant lead to inequivalence of tibial function among healthy young adults. *Journal of Bone and Mineral Research*, 2011, **26**(12): pp.2872–2885.

[16] Patton, D. M., Bigelow, E. M. R., *et al.* (2019) The relationship between whole bone stiffness and strength is age and sex dependent*. Journal of Biomechanics*, 2019, **83**: pp.125–133.

[17] Jepsen, K. J., Bigelow, E. M. R., Schlecht, S. H. (2015) Women Build Long Bones With Less Cortical Mass Relative to Body Size and Bone Size Compared With Men. *Clinical Orthopaedics and Related Research*, 2015, **473**(8): pp.2530–2539.

[18] Schlecht, S. H., Bigelow, E. M. R., Jepsen, K. J. (2015) How Does Bone Strength Compare Across Sex, Site, and Ethnicity? *Clinical Orthopaedics and Related Research*, 2015, **473**(8): pp.2540–2547.

[19] Schlecht, S. H., Bigelow, E. M. R., Jepsen, K. J. (2014) Mapping the natural variation in whole bone stiffness and strength across skeletal sites. *Bone*, 2014, **67**: pp.15–22.

[20] Griffon, D., Wallace, L., Bechtold, J. (1995) Biomechanical properties of canine corticocancellous bone frozen in normal saline solution. *American Journal of Veterinary Research*, 1995, **56**: p.822.

[21] Linde, F., Sorenson, H. C. (1993) The effect of different storage methods on the mechanical properties of trabecular bone. *Journal of Biomechanics*, 1993, **26**: p.1249.

[22] Reilly, D., Burstein, A. (1975) The elastic and ultimate properties of compact bone tissue. *Journal of Biomechanics*, 1975, **8**(6): pp.393–405.

[23] Hamer, A. J., Strachen, J. R., *et al.* (1996) Biomechanical properties of cortical allograft bone using a new method of bone strength measurement. A comparison of fresh, fresh-frozen, and irradiated bone. *Journal of Bone and Joint Surgery*, 1996, **78B**: p.363.

[24] Frankel, V. H. (1960) The Femoral Neck. Function, Fracture mechanism, Internal fixation. An experimental study. *Almqvist and Wiskell*, Goteborg, Sweden, 1960.

[25] Trafton, P. G. (1992) Skeletal Trauma: Fractures, Dislocations, Ligamentous Injuries, pp.1771–1869, *W B Saunders Co*, Philadelphia, PA, USA, 1992.

[26] Ivarsson, B. J., Manaswi,, A., *et al*. (2008) Site, type, and local mechanism of tibial shaft fracture in drivers in frontal automobile crashes. *Forensic Science International*, 2008, **175**: pp.186–192.

[27] Danelson, K. A., Kemper, A. R., *et al.* (2015) Comparison of ATD to PMHS Response in the Under-Body Blast Environment. *Stapp Car Crash Journal*, 2015, **59**(November 2015): pp.445–520.

[28] ASTM F382-99. (2003) Standard Specification and Test Method for Metallic Bone Plates. *ASTM International*, West Conshohocken, PA, USA, 2003.

[29] Ebacher, V., Tang, C., *et al.* (2007) Strain redistribution and cracking behavior of human bone during bending. *Bone*, 2007, **40**(5): pp.1265–1275.

[30] SAE. (2007) Instrumentation for impact test-part 1-electronic instrumentation, J211/1. 2007, Warrendale, PA, USA.

[31] Minitab 18 Statistical Software. (2020) *Minitab, Inc.*, State College, PA, USA, 2020.

[32] Tommasini, S. M., Nasser, P., Jepsen, K. J. (2007) Sexual dimorphism affects tibia size and shape but not tissue-level mechanical properties. *Bone*, 2007, **40**(2): pp.498–505.

[33] Hunter, R. L., Briley, K., Agnew, A. M. (2019) Sex Differences in Human Tibia Cortical Bone Morphometrics from Computed Tomography (CT). *Proceedings of IRCOBI Conference*, 2019, Florence, Italy.

[34] Nyquist, G. W., Cheng, R., El-Bohy, A. A. R., King, A. I. (1985) Tibia Bending: Strength and Response. SAE Technical Paper, 1985.

[35] Kerrigan, J. R., Bhalla, K. S., *et al.* (2003) Experiments for Establishing Pedestrian-Impact Lower Limb Injury Criteria. SAE Technical Paper, 2003.

[36] Kerrigan, J., Bhalla, K., Madeley, N., Crandall, J., Deng, B. (2003) Response Corridors for the Human Leg in 3-Point Lateral Bending. *Proceedings of the 7th US National Congress on Computational Mechanics*, 2003, Albuquerque, New Mexico, USA.

[37] Kerrigan, J. R., Drinkwater, D. C., *et al.* (2004) Tolerance of the human leg and thigh in dynamic latero-medial bending. *International Journal of Crashworthiness*, 2004, **9**(6): pp.607–623.

[38] Duren, D. L., Seselj, M., Froehle, A. W., Nahhas, R. W., Sherwood, R. J. (2013) Skeletal growth and the changing genetic landscape during childhood and adulthood. *American Journal of Physical Anthropology*, 2013, **150**(1): pp.48–57.

[39] Nieves, J. W., Formica, C., *et al*. (2005) Males have larger skeletal size and bone mass than females, despite comparable body size. *Journal of Bone and Mineral Research*, 2005, **20**(3): pp.529–535.

[40] Milgrom, C., Giladi, M., *et al.* (1989) The area moment of inertia of the tibia: A risk factor for stress fractures. *Journal of Biomechanics*, 1989, **22**(11/12): pp.1243–1248.

[41] Mo, F., Arnoux, P. J., Jure, J. J., Masson, C. (2012) Injury tolerance of tibia for the car-pedestrian impact. *Accident Analysis and Prevention*, 2012, **46**: pp.18–25.

VIII. APPENDIX

TABLE AI
POST-MORTEM HUMAN SUBJECT AND TIBIA LEVEL DATA

Test ID	Peak Force (kN)	Sex	Age (years)	Height (cm)	Weight (kg)	Side	Tibia Length (mm)
Tib001	12.7	Male	64	182.8	78.9	Right	411
Tib002	20.2	Male	63	185.4	88.4	Right	406
Tib003	16.6	Male	77	170.1	78.4	Right	366
Tib004	17.2	Female	84	167.6	51.2	Right	358
Tib005	15.4	Female	86	157.4	43.0	Right	358
Tib006	12.5	Female	102	149.8	37.4	Right	355
Tib007	19.3	Male	73	165.1	62.1	Right	365
Tib008	16.7	Male	74	180.3	63.5	Left	397
Tib009	18.6	Female	85	170.1	43.5	Left	359
Tib010	21.9	Female	89	152.4	55.7	Left	334

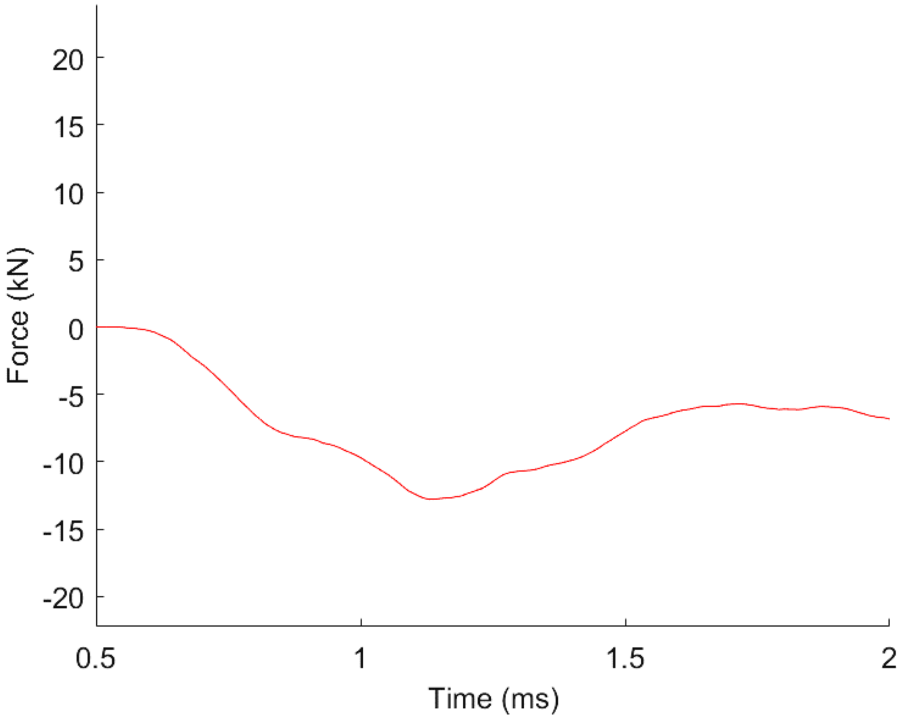

Fig. A1. Force-time plot for sample Tib001 using J211 coordinate system [30]

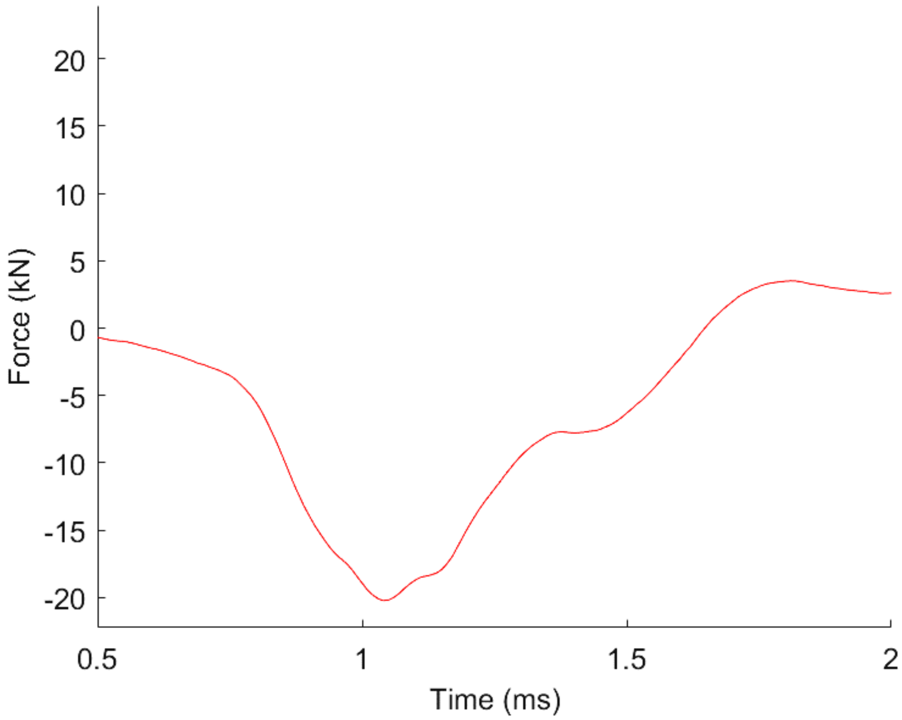

Fig. A2. Force-time plot for sample Tib002 using J211 coordinate system [30]

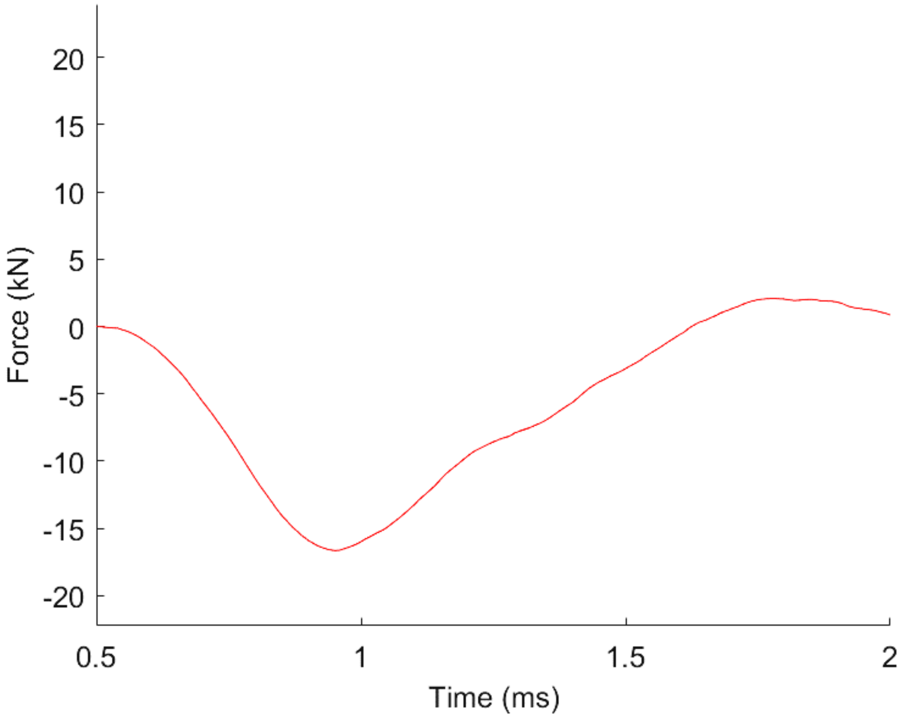

Fig. A3. Force-time plot for sample Tib003 using J211 coordinate system [30]

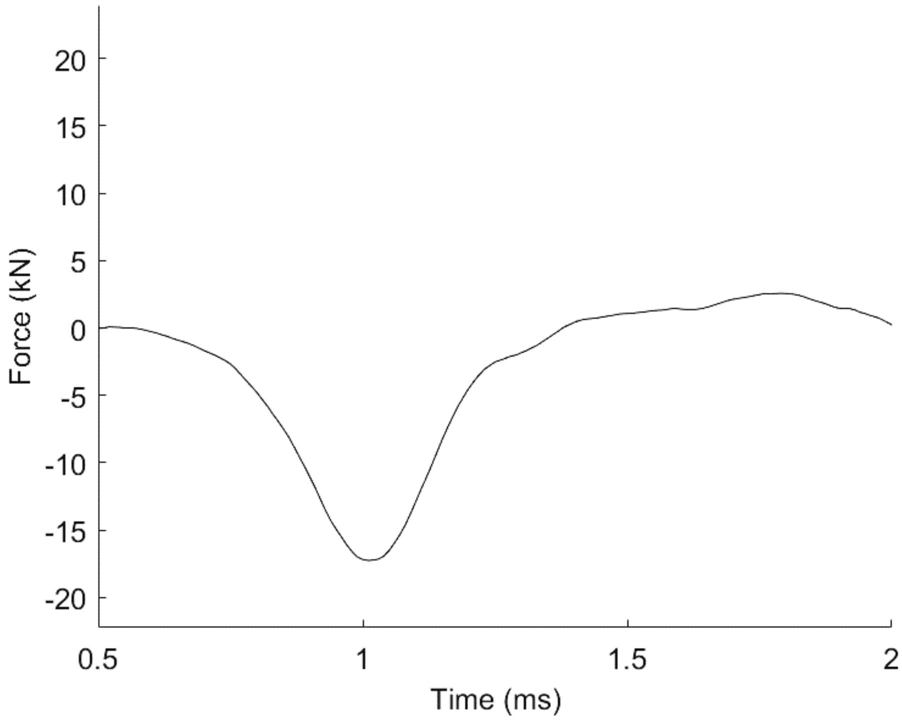

Fig. A4. Force-time plot for sample Tib004 using J211 coordinate system [30]

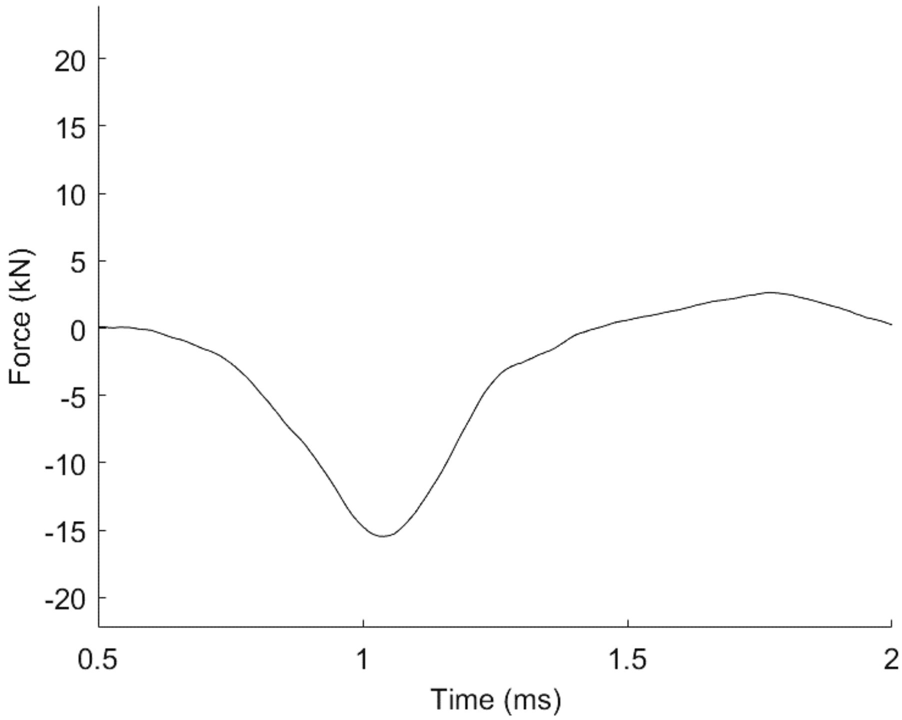

Fig. A5. Force-time plot for sample Tib005 using J211 coordinate system [30]

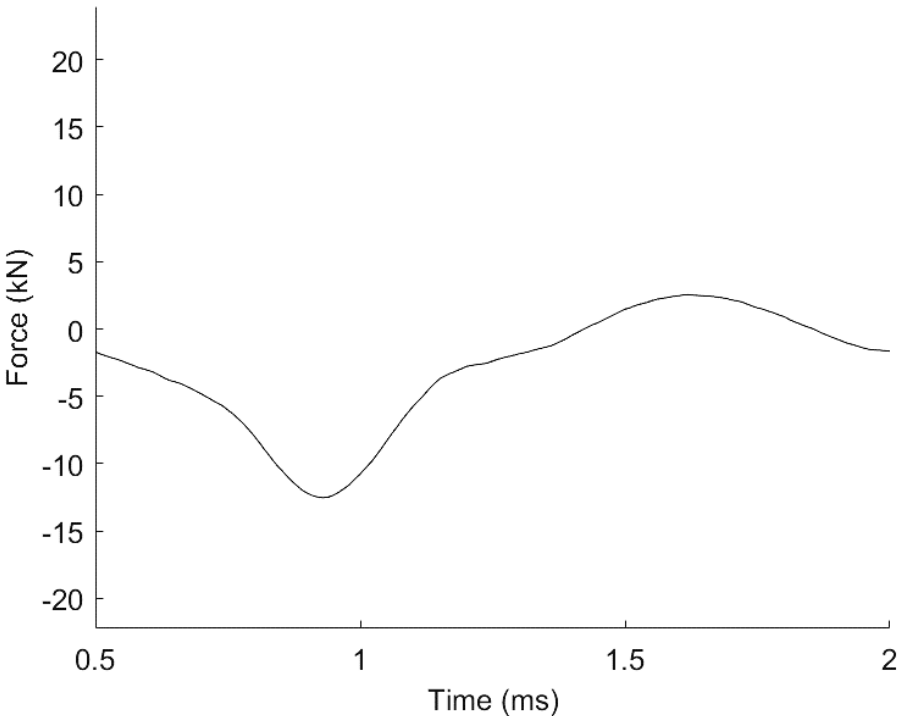

Fig. A6. Force-time plot for sample Tib006 using J211 coordinate system [30]

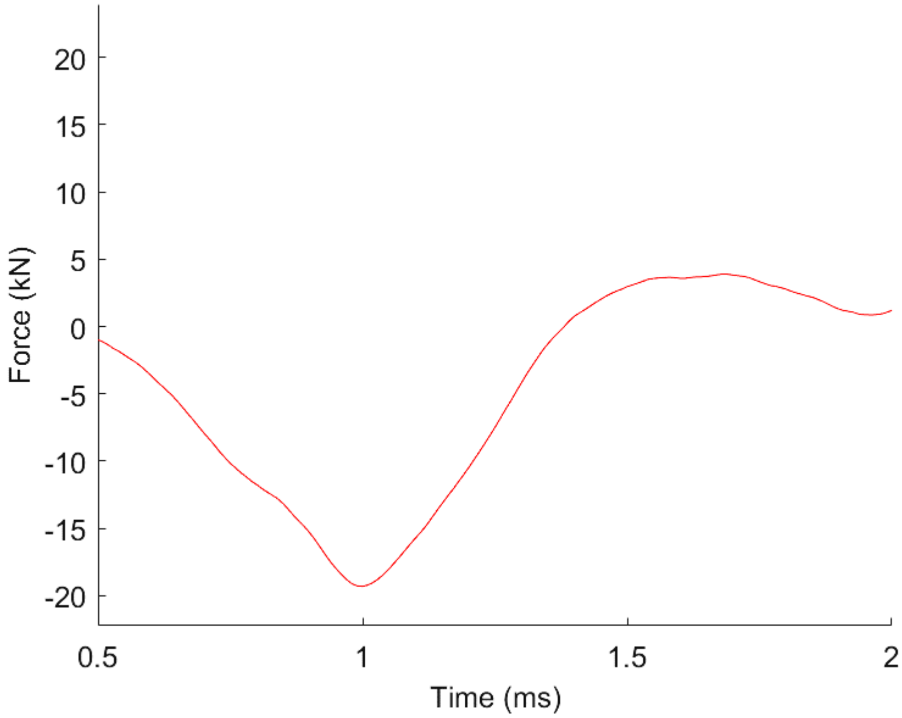

Fig. A7. Force-time plot for sample Tib007 using J211 coordinate system [30]

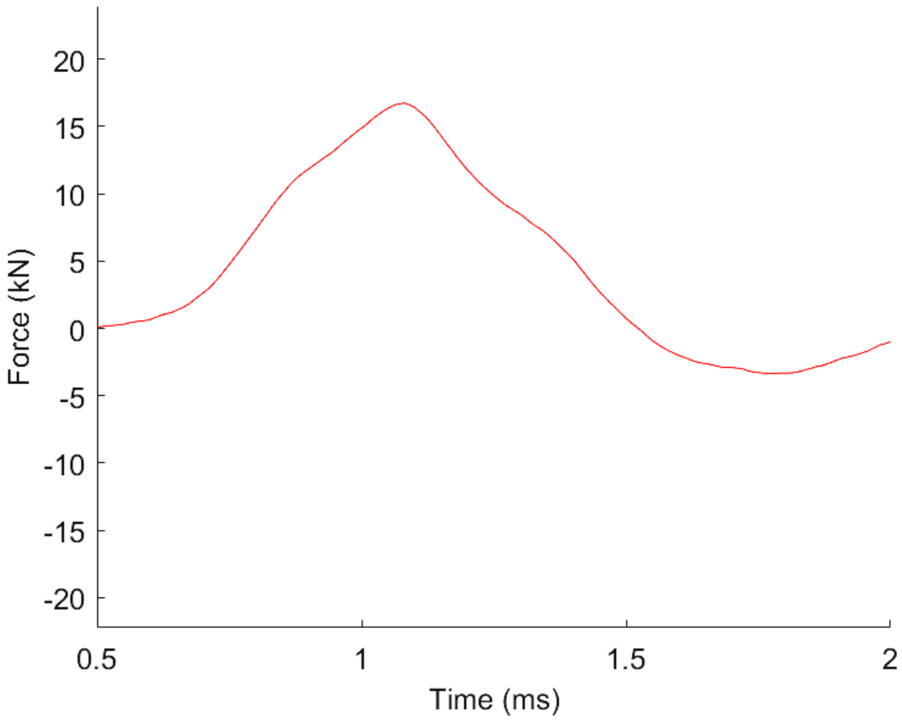

Fig. A8. Force-time plot for sample Tib008 using J211 coordinate system [30]

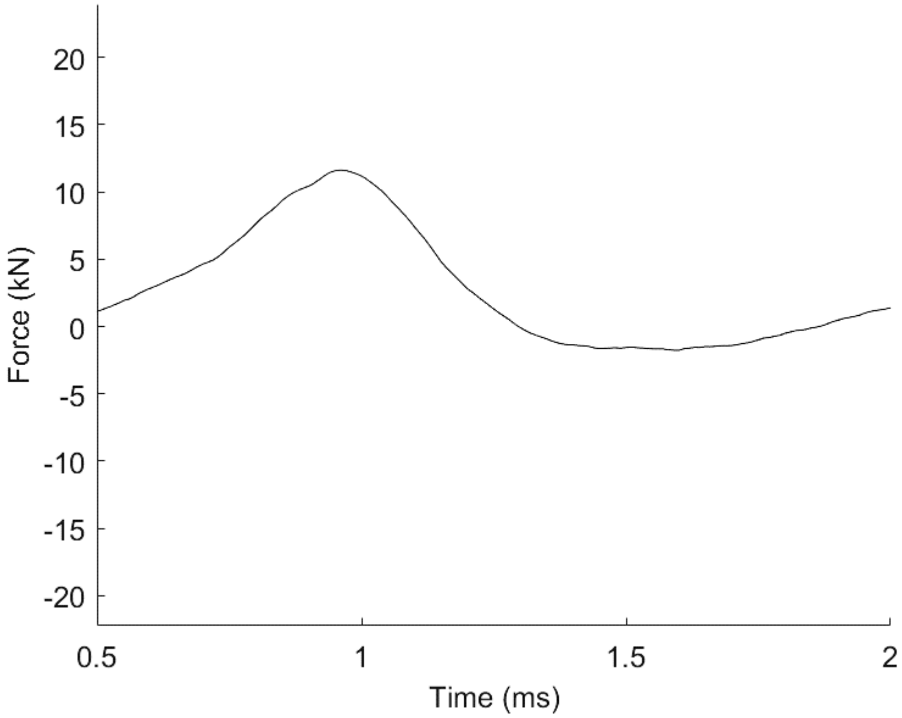

Fig. A9. Force-time plot for sample Tib009 using J211 coordinate system [30]

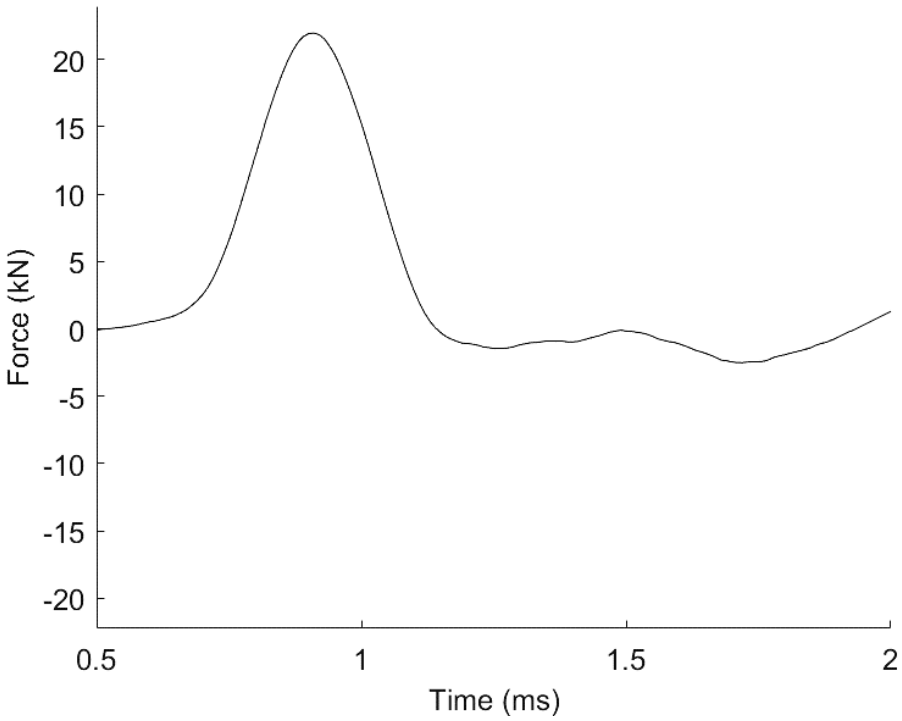

Fig. A10. Force-time plot for sample Tib010 using J211 coordinate system [30]